Natural Resources Canada
Ressources naturelles Canada

Preliminary characterization of metamorphism on Cumberland Peninsula, Baffin Island, Nunavut

B.M. Hamilton, D.R.M. Pattison, M. Sanborn-Barrie, and M.D. Young

Geological Survey of Canada
Current Research 2012-9

2012

Canada

Geological Survey of Canada
Current Research 2012-9

Preliminary characterization of metamorphism on Cumberland Peninsula, Baffin Island, Nunavut

B.M. Hamilton, D.R.M. Pattison, M. Sanborn-Barrie, and M.D. Young

2012

ISSN 1701-4387
Catalogue No. M44-2012/9E-PDF
ISBN 978-1-100-20959-3
doi:10.4095/291530

A copy of this publication is also available for reference in depository libraries across Canada through access to the Depository Services Program's Web site at http://dsp-psd.pwgsc.gc.ca

This publication is available for free download through GEOSCAN
http://geoscan.ess.nrcan.gc.ca/

Toll-free (Canada and U.S.A.): 1-888-252-4301

Recommended citation
Hamilton, B.M., Pattison, D.R.M., Sanborn-Barrie, M., Young, M.D., 2012. Preliminary characterization of metamorphism on Cumberland Peninsula, Baffin Island, Nunavut; Geological Survey of Canada, Current Research 2012-9, 17 p. doi: 10.4095/291530

Critical review
R. Berman

Authors
B.M. Hamilton (brett.hamilton@ucalgary.ca)
D.R.M. Pattison (pattison@ucalgary.ca)
Department of Geoscience
University of Calgary
2500 University Drive NW
Calgary, Alberta
T2B 1N4

M.D. Young(MDYoung@Dal.ca)
Dalhousie University,
Edzell Castle Circle
Halifax, Nova Scotia
B3H 4J1

M. Sanborn-Barrie (Mary.Sanborn-Barrie@NRCan-RNCan.gc.ca)
Geological Survey of Canada
601 Booth Street
Ottawa, Ontario
K1A OE8

Correction date:

Preliminary characterization of metamorphism on Cumberland Peninsula, Baffin Island, Nunavut

B.M.Hamilton, D.R.M. Pattison, M. Sanborn-Barrie, and M.D. Young

Hamilton, B.M., Pattison, D.R.M., Sanborn-Barrie, M., Young, M.D., 2012. Preliminary characterization of metamorphism on Cumberland Peninsula, Baffin Island, Nunavut; Geological Survey of Canada, Current Research 2012-9, 17 p. doi: 10.4095/291530

Abstract: A metamorphic map of Cumberland Peninsula, Nunavut is presented based on field and petrographic observations of metapelite, metapsammite, and metabasite. Five metamorphic zones are recognized in metapelite: staurolite+muscovite (lower-amphibolite facies); andalusite+muscovite; sillimanite+muscovite (both middle-amphibolite facies); sillimanite±K-feldspar (upper-amphibolite facies); and cordierite+garnet±K-feldspar (granulite facies). These subfacies comprise approximately 1%, 5%, 15%, 70%, and 9% of Cumberland Peninsula's metamorphic rocks, respectively. Most amphibolite-facies assemblages developed during Paleoproterozoic regional metamorphism. Lower- and middle-amphibolite-facies rocks occur in a 120 km by 15 km, structurally controlled corridor. Sillimanite+muscovite zone rocks had sequential growth of staurolite, andalusite, then sillimanite. Both the sillimanite+muscovite prograde P-T path and the piezothermic array for the area transect the staurolite+andalusite stability field with a shallow P/T slope implying middle-amphibolite-facies metamorphism took place at low pressure (3.3–4.1 kbar). Porphyroblasts in amphibolite-facies rocks are mostly intertectonic with respect to two phases of Paleoproterozoic deformation suggesting regional metamorphism was orogenic. Two styles of granulite-facies metamorphism occurred prior to regional metamorphism. The first comprises a southeastern domain of granulite-facies rocks variably overprinted by amphibolite-facies metamorphism. The second formed later in close proximity to widely dispersed charnockitic plutons, suggesting regional contact metamorphism.

Résumé : Nous présentons une carte métamorphique de la péninsule Cumberland (Nunavut) fondée sur des observations sur le terrain ainsi que des observations pétrographiques de métapélites, de métapsammites et de métabasites. On reconnaît cinq zones métamorphiques dans les métapélites : staurotide+muscovite (faciès des amphibolites inférieur), andalousite+muscovite ainsi que sillimanite+muscovite (toutes deux du faciès des amphibolites intermédiaire), sillimanite±feldspath potassique (faciès des amphibolites supérieur) et cordiérite+grenat±feldspath potassique (faciès des granulites). Ces sous-faciès se partagent respectivement environ 1 %, 5 %, 15 %, 70 % et 9 % des roches métamorphiques de la péninsule Cumberland. La plupart des associations minérales du faciès des amphibolites se sont formées lors d'un épisode de métamorphisme régional au Paléoprotérozoïque. Les roches du faciès des amphibolites inférieur et intermédiaire se situent dans un corridor à contrôle structural de 120 km sur 15 km. Les roches de la zone à sillimanite+muscovite rendent compte d'une croissance séquentielle s'amorçant par la staurotide, passant à l'andalousite, puis se terminant par la sillimanite. Le chemin P-T prograde de la zone à sillimanite+muscovite ainsi que le tracé de la séquence piézothermique de la région traversent le champ de stabilité des phases staurotide+andalousite avec une faible pente P/T, ce qui laisse supposer que le métamorphisme au faciès des amphibolites intermédiaire s'est déroulé à faible pression (3,3-4,1 kbar). Les porphyroblastes dans les roches du faciès des amphibolites sont, pour la plupart, d'origine intertectonique, en référence aux deux phases de déformation du Paléoprotérozoïque, ce qui donne à penser que le métamorphisme régional est de nature orogénique. Deux styles de métamorphisme au faciès des granulites se sont produits avant le métamorphisme régional. Le premier se reconnaît dans un domaine sud-est de roches du faciès des granulites, qui portent en surimpression les effets variables d'un métamorphisme au faciès des amphibolites. Le second s'est formé ultérieurement à proximité de plutons charnockitiques largement dispersés, suggérant un métamorphisme de contact à l'échelle régionale.

INTRODUCTION

The main Precambrian tectonic elements in northeast Canada are Archean cratons and microcontinents, and Paleoproterozoic marginal sequences, magmatic arcs, and collisional orogenic belts that form part of the Trans-Hudson Orogen (Hoffman, 1988; St-Onge et al., 2007; Corrigan et al., 2009). Cumberland Peninsula, southeast Baffin Island, Nunavut (Fig. 1) has some of these elements; however, its cratonic affinity is uncertain, as is the orogeny responsible for deformation, metamorphism, and magmatism. New bedrock mapping on Cumberland Peninsula (Fig. 1; Sanborn-Barrie et al., 2011a, b, c, in press a, in press b; Sanborn-Barrie and Young, in press a, in press b, in

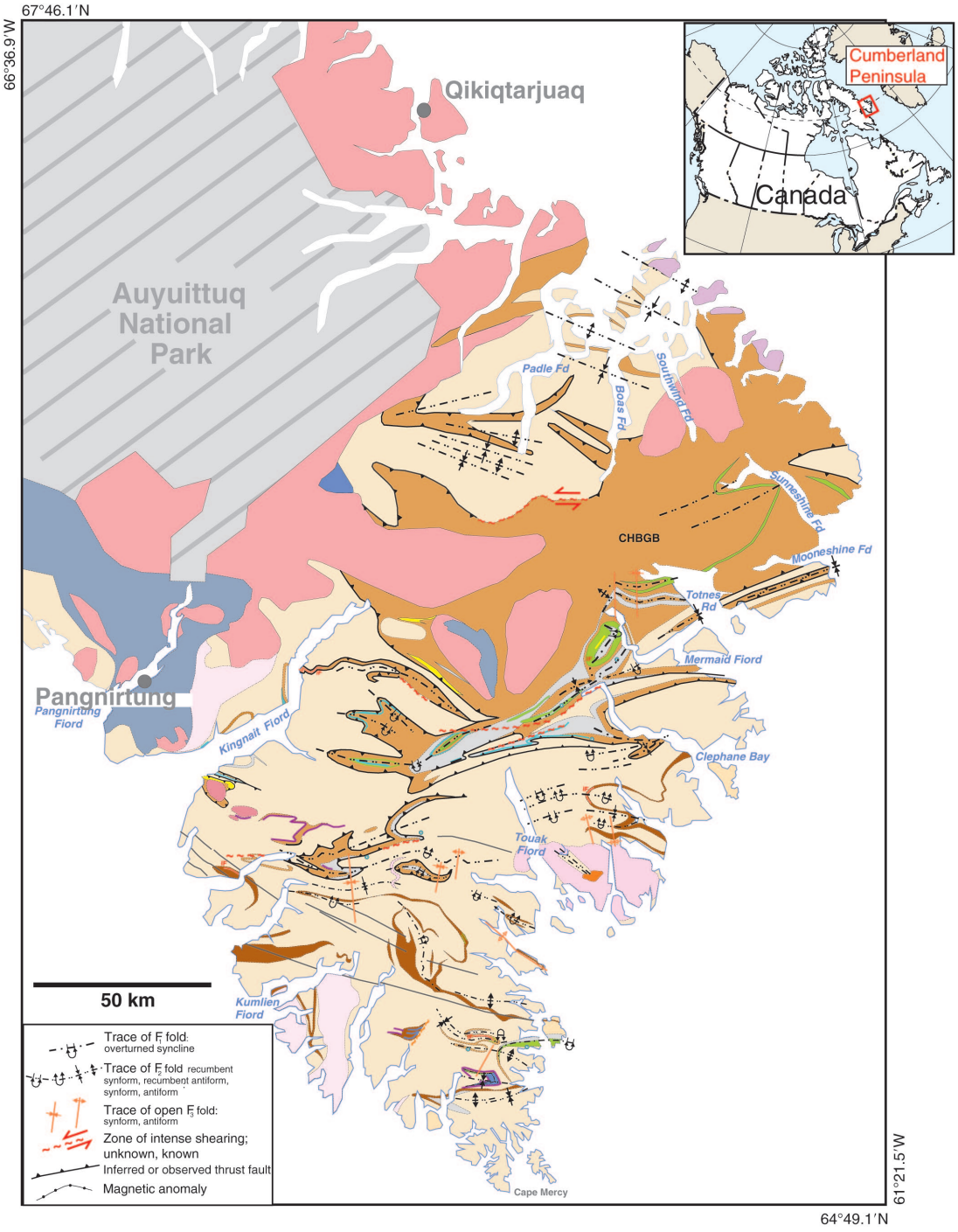

Figure 1. Geological map of Cumberland Peninsula, *modified from* Sanborn-Barrie and Young (2011). CHBGB = central Hoare Bay group belt. *See* legend next page

press c) documents the geology of this region, which facilitates an understanding of the geological evolution and constrains tectonic models. This contribution presents a new map of metamorphic mineral assemblage zones for Cumberland Peninsula (Fig. 2, 3), expanding on the reconnaissance studies of Fraser et al. (1978) and Jackson and Morgan (1978). Fieldwork was conducted during a mapping program from 2009 to 2011 as a part of Natural Resources Canada's Geo-Mapping for Energy and Minerals (GEM) Cumberland Peninsula Multiple Metals project. Laboratory work in 2010 and 2011 at the University of Calgary augmented the fieldwork and together comprises the first part of B. Hamilton's Ph.D. research on the metamorphic geology of Cumberland Peninsula.

PHANEROZOIC

Tertiary basalt flows and flat-lying metasedimentary rocks.

NEOPROTEROZOIC

Diabase dyke.

PALEOPROTEROZOIC

INTRUSIVE ROCKS

QIKIQTARJUAQ SUITE ca. 1.9–1.89 Ga

Orthopyroxene±garnet granodiorite-monzogranite (charnockite)-quartz monzonite, variably K-feldspar megacrystic.

Orthopyroxene quartz diorite±tonalite.

Pyroxenite sill: clinopyroxene-phyric.

SUPRACRUSTAL ROCKS

Semipelite±psammite±siltstone.

Psammite±semipelite±quartzite.

Iron-formation: oxide- and silicate-facies.

Shale, chert±siltstone: black, graphitic, commonly sulphidic.

Quartzite: pink, hematized, orthoquartzite.

Ultramafic-mafic volcanic rocks.

Marble-calc-silicate±semipelite.

Quartzite, limy arenite: white-grey-weathering.

PALEOPROTEROZOIC/ARCHEAN

Granodiorite: orthopyroxene-biotite-magnetite, brown fresh surface, locally quartz-porphyritic.

Tonalite: variably foliated, biotite-bearing.

ARCHEAN

Biotite±garnet granodiorite.

K-feldspar porphyritic charnockite.

Tonalite: variably foliated to gneissic tonalite with gabbro and metasedimentary inclusions, cut by monzogranite-quartz diorite. May include diorite, quartz diorite.

Semipelite-psammite±pillow basalt±quartz porphyry.

GEOLOGY OF CUMBERLAND PENINSULA

This section summarizes the regional geology of Cumberland Peninsula (Fig. 1) based on recent geological (Sanborn-Barrie and Young, 2011, in press a, in press b, in press c; Sanborn-Barrie et al., 2011a, b, c, in press a, in press b), geochronological (Rayner et al., in press), and geochemical (Whalen et al., in press) studies. The main lithological components include 1) extensive, variably foliated to gneissic, Mesoarchean to Neoarchean tonalite-granodiorite of the Archean plutonic gneiss complex, which includes thin layers of mafic igneous rocks and Archean supracrustal rocks; 2) discrete Neoarchean granodiorite-monzogranite-charnockite plutons; 3) a Paleoproterozoic clastic-dominated supracrustal sequence, designated the Hoare Bay group (Jackson, 1971; Jackson and Taylor, 1972), now recognized to underlie the majority of the central and eastern parts of the peninsula; and 4) the Paleoproterozoic monzogranite-charnockite-diorite Qikiqtarjuaq plutonic suite, which is typically orthopyroxene- and/or garnet-bearing. The continuous domain of Hoare Bay group rocks is referred to here as the central Hoare Bay group belt (Fig. 1). All of the rocks discussed in this paper have been metamorphosed during the Paleoproterozoic, but the 'meta' prefix has been omitted from all rock types for brevity.

The most conspicuous structures in Cumberland Peninsula are mesoscopic to map-scale F_2 folds. They generally verge south, plunge shallowly to the west, have a close to isoclinal tightness, and a similar style. In Paleoproterozoic pelitic rocks, bedding-parallel schistosity is folded in F_2 folds and axial-planar schistosity is rare. Contacts between the Archean plutonic gneiss complex and the Hoare Bay group are tectonic and interpreted to be mainly the result of thrust faulting. Mylonitic rocks along the central Hoare Bay group belt–Archean plutonic gneiss complex contact are thought to represent east-west D_2 shear zones. As Archean plutonic gneiss complex–Hoare Bay group contacts are folded by F_2 folds, thrusting occurred prior to folding. Deformation associated with thrust faulting may be responsible for the development of the early schistosity, which was tightened and folded during F_2 folding.

The metamorphic geology can be divided into lower-, middle-, and upper-amphibolite facies, and granulite facies. Each subfacies is described below. Tertiary volcanic and sedimentary rocks and Neoproterozoic diabase dykes are not dealt with in detail; however, field observations suggest they are subgreenschist facies (cf. Fraser et al., 1978).

METHODS

Mineral assemblage mapping

The metamorphic map for Cumberland Peninsula is based upon peak-temperature metamorphic silicate mineral assemblages. Mineral assemblages were identified based on field observations and thin-section examination. The

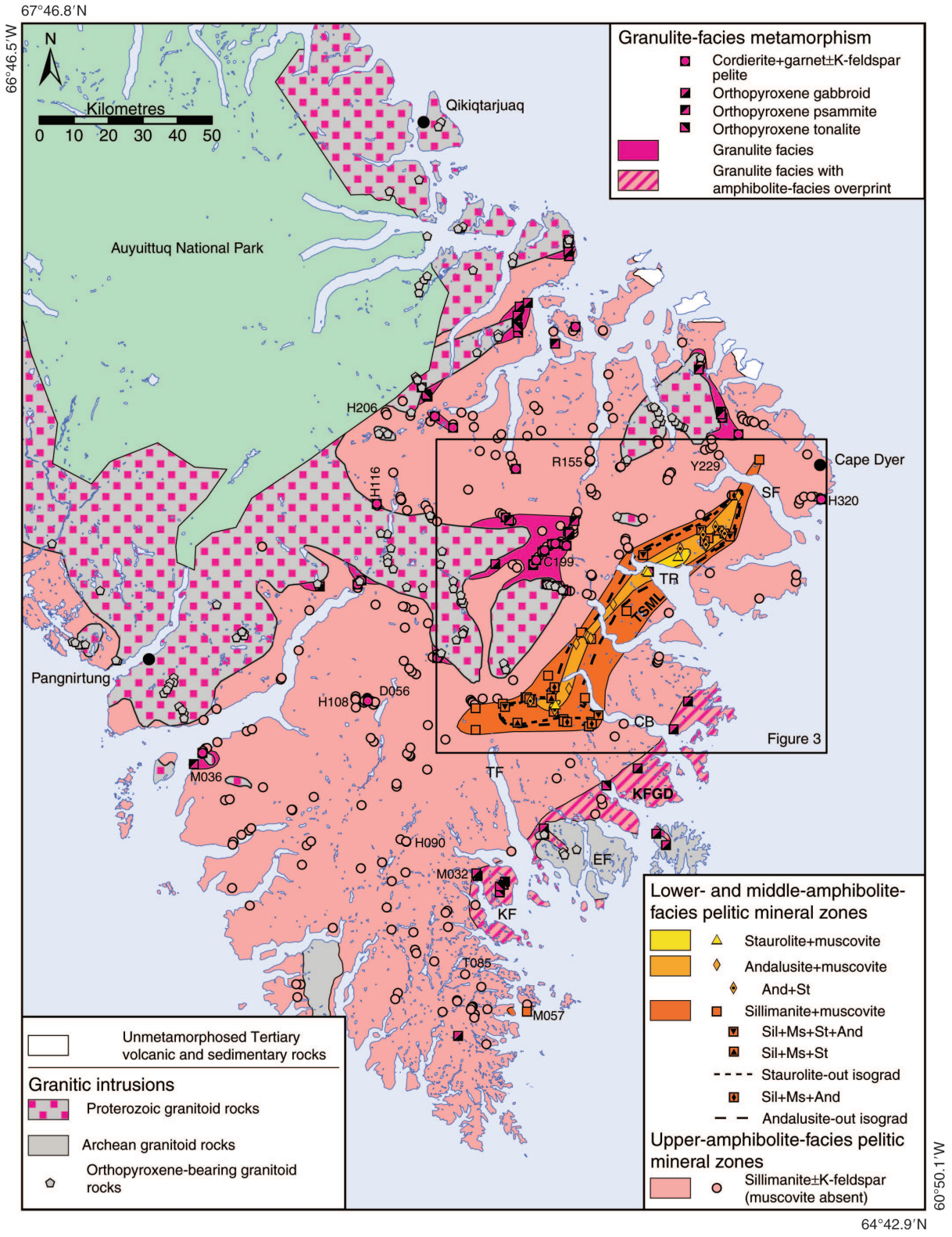

Figure 2. Metamorphic map of Cumberland Peninsula with sample localities discussed in the text. CB = Clephane Bay, EF = Exaluin Fiord, KF = Kairolik Fiord, KFGD = Kairolik Fiord granulite domain, SF = Sunneshine Fiord, TF = Touak Fiord, TR = Totnes Road, TSML = Touak-Sunneshine metamorphic low; Sil = sillimanite, Ms = muscovite, St = staurolite, And = andalusite.

metamorphic map is preliminary, as some samples collected in 2010 and 2011 have not yet been examined petrographically. In particular, K-feldspar identification is generally only reliable with sodium cobaltinitrite staining, which has only been performed on select samples. The presence of crystallized partial melt has not been mapped at this time. Delineation of metamorphic zones was largely based on mineral assemblages observed in pelitic rocks and gabbroic rocks (Fig. 2, 3). The metamorphic zones correlate with metamorphic facies using common literature definitions (Table 1, 2; e.g. Miyashiro (1994); Spear (1993)).

Thermodynamic modelling

Preliminary thermodynamic modelling of pelitic samples was carried out to constrain the pressure-temperature (P-T) conditions of each mineral zone. Equilibrium assemblage diagrams were calculated in the chemical subsystem MnO-Na_2O-CaO-K_2O-FeO-MgO-Al_2O_3-SiO_2-H_2O-TiO_2±Fe_2O_3 using an updated version of the Holland and Powell (1998) thermodynamic data set (version 5.5, November 2003), and the mineral activity-composition models described and referenced in Stowell et al. (2011). The calculations were performed using the software Theriak/Domino (de Capitani and

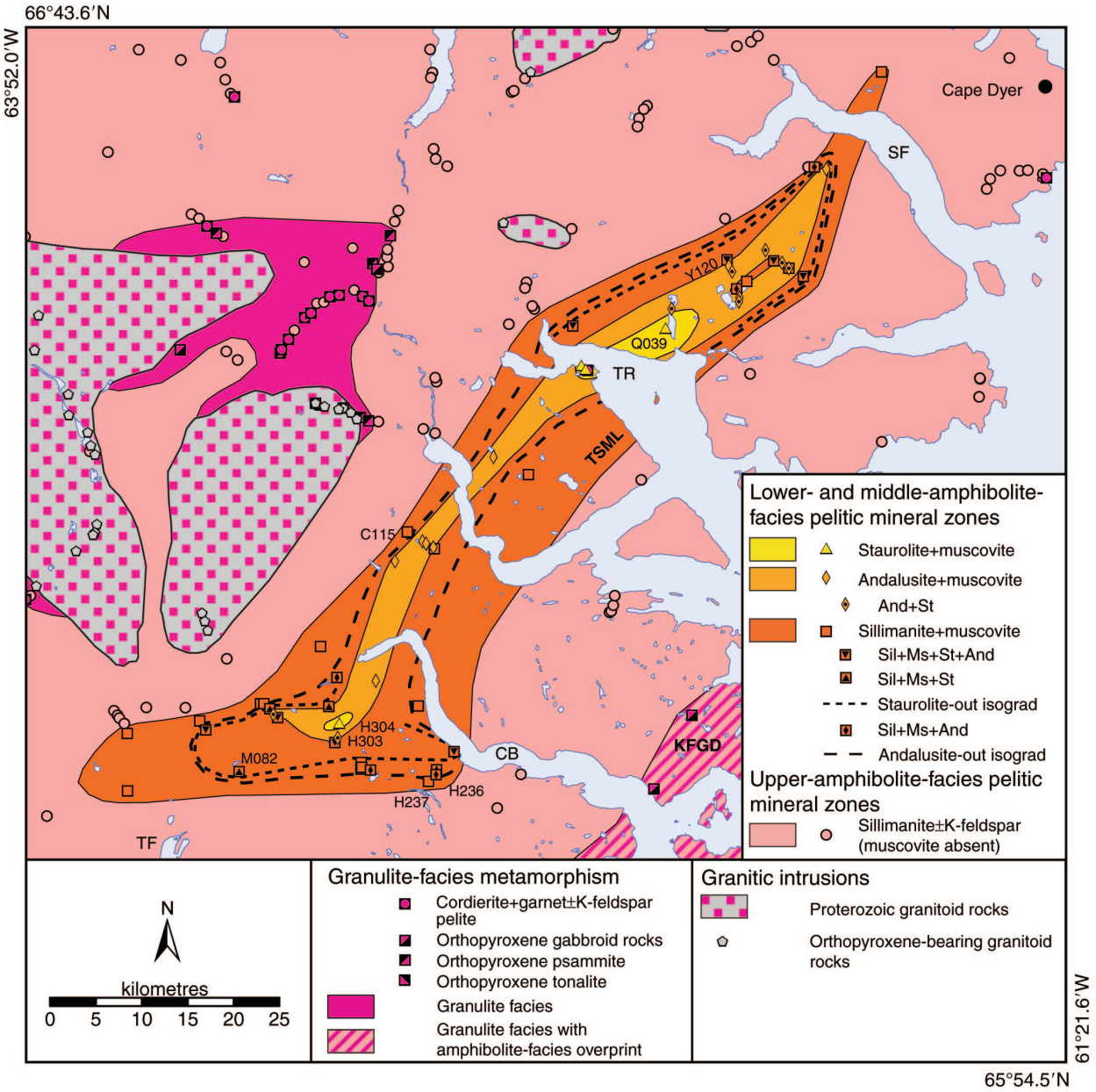

Figure 3. Metamorphic map of the Touak-Sunneshine metamorphic low. CB = Clephane Bay, KFGD = Kairolik Fiord granulite domain, SF = Sunneshine Fiord, TR = Totnes Road, TSML = Touak-Sunneshine metamorphic low; And = andalusite, St = staurolite, Sil = sillimanite, Ms = muscovite.

Brown, 1987; de Capitani and Petrakakis, 2010). The composition of bulk-rock samples was determined at the McGill University Trace Element Analytical Laboratories using a Philips PW2440 4 kW X-ray fluorescence spectrometer system; C and S were measured by LECO combustion-infrared absorption spectroscopy (Table 3).

LOWER- AND MIDDLE-AMPHIBOLITE FACIES

Lower- and middle-amphibolite facies, muscovite-bearing assemblages in pelitic rocks define a 120 km long and 15 km wide, northeast-trending corridor that extends from Touak Fiord to Sunneshine Fiord, herein termed the 'Touak-Sunneshine metamorphic low' (Fig. 2, 3). Within the map area, this corridor contains rocks that record the lowest strain, in which primary volcanic and sedimentary textures are observed (Keim et al., 2011). Primary textures are rarely recognized outside of the Touak-Sunneshine metamorphic low.

Three approximately concentric zones, separated by isograds, are recognized within the Touak-Sunneshine metamorphic low, with the lowest grade in the centre. The isograds are mostly subparallel to the trend of geological map units (compare Fig. 1 and 2). In detail, however, isograds crosscut lithological boundaries. For example, the southern margin of the central Hoare Bay group belt changes from middle-amphibolite facies in the Touak-Sunneshine metamorphic low to upper-amphibolite facies along strike to the southwest.

Staurolite+muscovite zone

The lowest grade zone within the Touak-Sunneshine metamorphic low is the staurolite+muscovite zone, most abundantly developed near Totnes Road. A single staurolite+muscovite zone outcrop was identified 45 km to the southwest near Clephane Bay (Fig. 3). Pelitic schist contains the assemblages staurolite+muscovite+biotite+plagioclase+quartz and chlorite+staurolite+muscovite+biotite+garnet+plagioclase+quartz (Fig. 4a). Subidioblastic staurolite porphyroblasts are honey coloured or brown in outcrop,

Table 1. Pelitic metamorphic zones and metamorphic facies.

Pelite metamorphic zone	Metamorphic facies
Staurolite+muscovite	Lower amphibolite
Andalusite+muscovite	Middle amphibolite
Sillimanite+muscovite	Middle amphibolite
Sillimanite±K-feldspar	Upper amphibolite
Cordierite+garnet±K-feldspar	Granulite

Table 2. Upper-amphibolite- and granulite-facies assemblages for various protoliths.

Protolith	Upper amphibolite facies	Granulite facies
Mafic igneous	Hbl+Pl±Qtz±Bt±Cpx±Grt	Opx+Hbl+Pl±Cpx±Qtz Cpx+Grt+Hbl+Pl±Qtz*
Psammite	Bt+Pl+Qtz±Sil	Opx±Bt+Pl+Qtz
Pelite	Bt+Grt+Sil±Kfs+Pl+Qtz	Crd+Grt+Sil±Bt±Spl±Opx+Pl+Qtz
Tonalite	Bt+Pl+Qtz±Kfs	Opx±Bt+Pl+Qtz±Kfs
		Cpx+Pl+Qtz±Kfs*
* These assemblages do not define granulite facies, but are observed with other granulite-facies rocks.		

Table 3. Whole-rock chemical composition of representative samples from Cumberland Peninsula.

Sample	SiO_2	TiO_2	Al_2O_3	$Fe_2O_3^T$	MnO	MgO	CaO	Na_2O	K_2O	P_2O_5	CO_2	SO_3	LOI	Total
09SRB-H090B	57.06	0.91	24.56	9.37	0.14	2.37	0.53	1.20	2.92	0.024	0.64	0.05	1.12	100.41
09SRB-H108B	58.54	1.09	23.01	10.40	0.12	2.06	0.32	0.50	3.00	0.096	<dl	0.06	0.99	100.27
09SRB-T085A	60.69	0.70	20.05	6.99	0.10	3.07	0.39	0.66	5.57	0.100	1.93	0.06	1.97	100.51
All constituents are reported as weight per cent; $Fe_2O_3^T$ is an expression of total iron; <dl – below detection limit.														

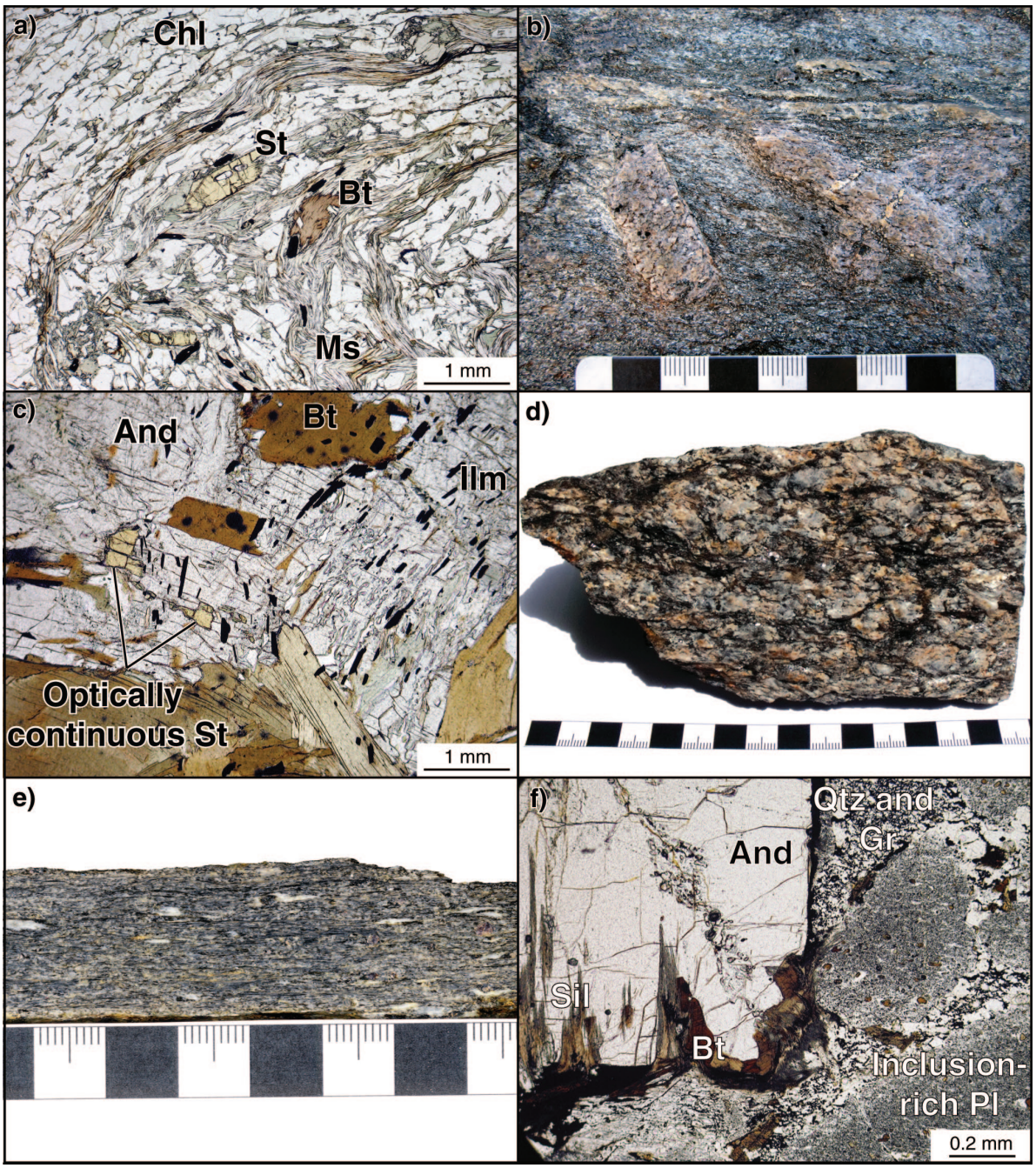

Figure 4. a) Photomicrograph of staurolite+muscovite zone chlorite+muscovite+biotite+staurolite+garnet+plagioclase+quartz pelitic schist. Prograde chlorite and muscovite define a folded (F_2) schistosity (S_1; 10SRB-H304A;) 2012-024. **b)** Photograph of andalusite+muscovite zone outcrop with pink andalusite porphyroblasts; scale in centimetres (10SRB-H303A;) 2012-029. **c)** Photomicrograph of andalusite+muscovite zone sample with the assemblage muscovite+biotite+andalusite+staurolite+garnet+plagioclase+quartz. Staurolite inclusions in andalusite are optically continuous and resorbed, suggesting that andalusite was partially produced from the breakdown of staurolite. Aligned ilmenite and quartz inclusions in andalusite (S_1) are oblique to external schistosity (S_2), although S_2 is not visible in this field of view (10SRB-H303A) 2012-031. **d)** Sillimanite+muscovite zone sample with relict andalusite porphyroblasts and the assemblage muscovite+biotite+sillimanite+andalusite+plagioclase+quartz; scale in centimetres (10SRB-H236C) 2012-018. **e)** Sillimanite+muscovite zone schist with the assemblage muscovite+biotite+sillimanite+garnet+plagioclase+quartz collected 750 m along tectonic strike from 10SRB-H236C; scale in centimetres (10SRB-H237C) 2012-012. **f)** Andalusite partially replaced by biotite and needles of sillimanite in andalusite+sillimanite+biotite+plagioclase+quartz psammite (10SRB-C115A) 2012-020. Chl = chlorite, St = staurolite, Bt = biotite, Ms = muscovite, And = andalusite, Ilm = ilmenite, Sil = sillimanite, Qtz = quartz, Gr = graphite, Pl = plagioclase.

typically 0.5–2 mm long, rarely up to 8 mm (Fig. 4a), and are prismatic to equant, occasionally with penetration twins. The locality near Clephane Bay is unique because it contains garnet and chlorite. Garnet is 1–2 mm, pink, idioblastic porphyroblasts. Chlorite and muscovite define a schistosity and are folded, suggesting a prograde origin.

Andalusite+muscovite zone

Pelitic rocks of the andalusite+muscovite zone have the assemblage andalusite+muscovite+biotite±staurolite±garnet +plagioclase+quartz. These pelitic rocks are porphyroblastic schist that contain pink, grey, or black rectangular andalusite prisms (Fig. 4b). Crystals are typically 1–4 cm long, with some examples over 20 cm long. Pink or red idioblastic or subidioblastic garnet, 1–3 mm in diameter, is found locally. Staurolite is similar to that found in the staurolite+muscovite zone, and occurs commonly in the matrix and as inclusions in andalusite (Fig. 4c) or rarely garnet.

Sillimanite+muscovite zone

The sillimanite+muscovite zone contains pelite with the assemblage sillimanite+muscovite+biotite±andalusite± staurolite±garnet+plagioclase+quartz. The first (i.e. lowest grade) occurrence of sillimanite is fibrolite, identified petrographically in rocks that, in the field, are indistinguishable from andalusite+muscovite zone samples (Fig. 4d). As the abundance of sillimanite increases, it occurs as monomineralic or sillimanite+biotite+quartz aggregates (Fig. 4e). Moving upgrade, the staurolite-out isograd is followed by the andalusite-out isograd.

Petrogenesis of sillimanite+muscovite zone pelite

The petrogenetic sequence for middle-amphibolite facies pelite is established by the following textures in sillimanite+muscovite zone samples: staurolite inclusions (sometimes corroded) in andalusite (Fig. 4c); sillimanite-bearing rocks with corroded andalusite rimmed by coarse-grained, randomly oriented muscovite with or without intergrown fibrolite; and andalusite partially replaced by sillimanite in muscovite-absent rocks (Fig. 4f). The first observation suggests staurolite grew prior to, or coevally with andalusite growth, and in some cases was partially consumed as andalusite grew. A reaction such as staurolite+muscovite+quartz = garnet +biotite+andalusite+H_2O (Spear, 1993) may be responsible for andalusite crystallization. The second observation is interpreted as evidence of a fluid-mediated ionic-exchange reaction from andalusite to sillimanite (Carmichael, 1969), although some of the muscovite may be retrograde in origin. The third observation indicates that sillimanite replaced andalusite in a direct polymorphic conversion. Therefore, the mineral growth sequence for rocks in the sillimanite+muscovite zone is staurolite, followed by andalusite, followed in turn by sillimanite, the same as the mapped order of the mineral assemblage zones.

UPPER-AMPHIBOLITE FACIES, SILLIMANITE±K-FELDSPAR ZONE

The majority of pelitic sedimentary rocks mapped on Cumberland Peninsula contain the upper-amphibolite-facies assemblage biotite+sillimanite+garnet±K-feldspar+ plagioclase+quartz (Fig. 2). Pelite in this zone is biotite±sillimanite schist, some of which is migmatitic (Fig. 5; Brown (1973)). Migmatitic rocks are usually stromatic metatexite with less than 10% leucosome (Fig. 5a), but some have patch-structured leucosome that crosscuts the foliation (Fig. 5b). The majority of pelite samples in this zone do not contain K-feldspar (Fig. 5a, b, c, d) and a number of K-feldspar-absent samples contain medium- or coarse-grained lenticular plagioclase+quartz leucosome (Fig. 5a). Where K-feldspar is observed, it occurs almost exclusively in plagioclase+quartz+K-feldspar leucosome (Fig. 5e) associated with myrmekitic plagioclase+quartz intergrowths. Pink or red subidioblastic garnet from 2 mm to 20 mm is common in both leucosome and melanosome. Garnet in leucosome is typically coarser than in the matrix. Sillimanite is more abundant in melanosome and occurs in fibrolitic or prismatic forms. The prismatic variety is typically 1–3 mm in length. Both varieties occur as monomineralic aggregates (Fig. 5b, c) or intergrown with biotite (Fig. 5a, e). A number of samples contain medium- to coarse-grained muscovite associated with sillimanite that is randomly oriented and interpreted to be late with respect to the biotite+sillimanite schistosity.

Migmatitic textures suggest some pelitic rocks underwent partial melting. Some pelitic rocks are migmatitic, whereas psammitic rocks are not. This observation supports anatexis as a migmatite-forming mechanism. Diffuse boundaries between trondhjemitic leucocratic segregations and melanosome (Fig. 5b) are interpreted as the result of in situ anatexis. In some places, mainly on the west side of the map area, leucosome-rich pelitic rocks grade into garnetiferous granite (Fig. 5f), suggesting some granitic liquid was sourced locally. Where garnet occurs preferentially in leucosome, it is interpreted as peritectic in origin. Leucocratic segregations are commonly folded (Fig. 5a, *see also* Fig. 7d) and deformation during and after partial melting may have squeezed melt from the source and obscured migmatitic textures.

Not all leucocratic segregations in the area have an anatectic origin. Quartz+plagioclase segregations occur in some muscovite+biotite schist in the andalusite+muscovite and sillimanite+muscovite zones, which likely formed by subsolidus tectonic segregation (Sawyer and Robin, 1986). Higher grade rocks also likely contain subsolidus segregations that formed on the prograde path. Granitoid veins were injected

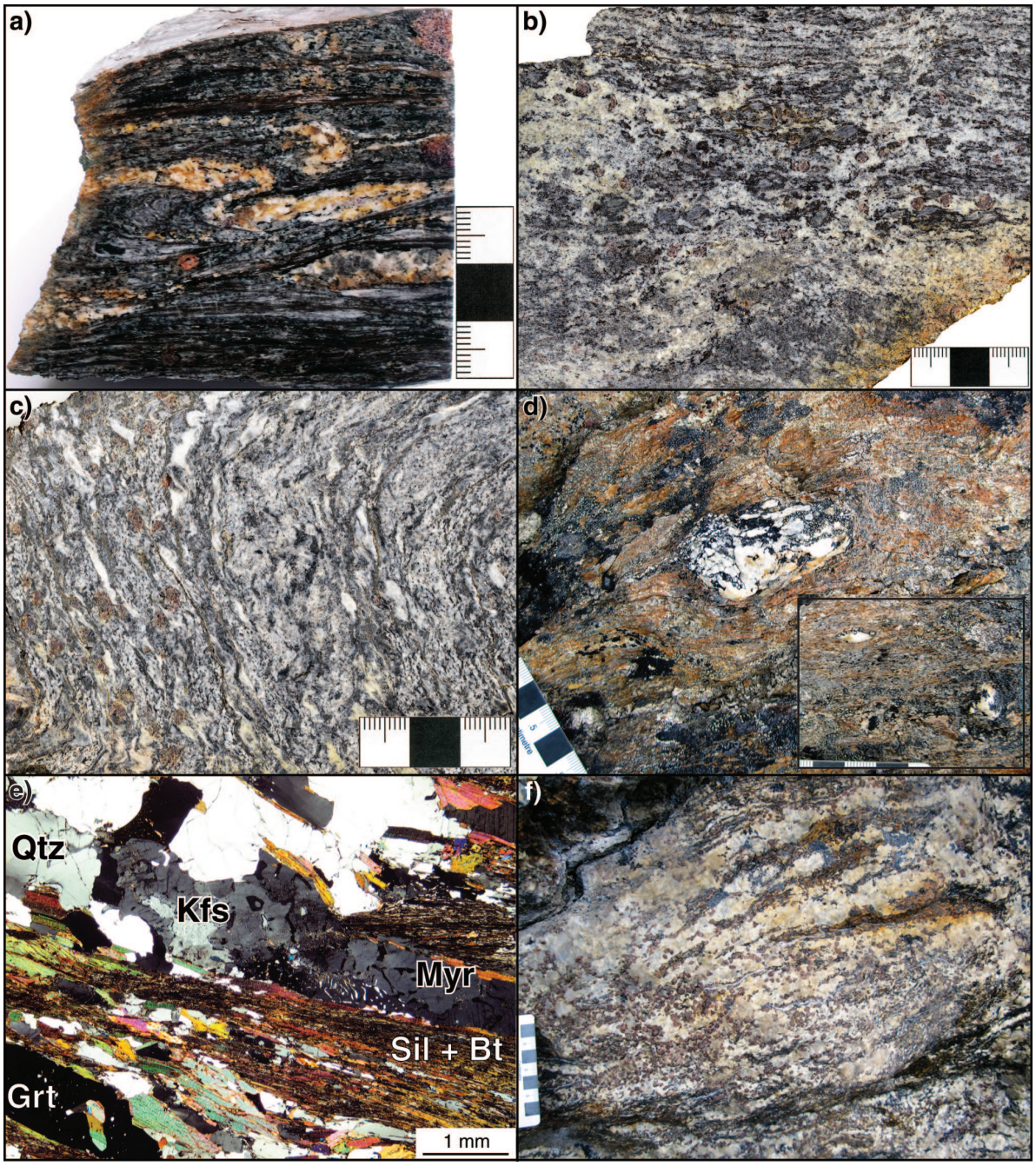

Figure 5. Sillimanite±K-feldspar zone rocks from Cumberland Peninsula. **a)** Biotite+sillimanite +garnet+plagioclase+quartz schist with folded (F_2) stromatic trondhjemitic leucosome; scale in centimetres (09SRB-H108B) 2012-025. **b)** Trondhjemite leucosome with diffuse boundaries is both foliation parallel and crosscutting in biotite+sillimanite+garnet+plagioclase+quartz schist; scale in centimetres (10SRB-Y229A) 2012-026. **c)** Nonmigmatitic biotite+sillimanite±garnet+ plagioclase+quartz schist with pelitic and semipelitic layers. Sillimanite forms discrete white knots; scale in centimetres (10SRB-H320A) 2012-027. **d)** Biotite+sillimanite±garnet+plagioclase+ quartz schist with tectonic inclusions of pegmatitic granite and (inset) two coarse-grained K-feldspar crystals; scale in centimetres (10SRB-R155A) 2012-030, 2012-017. **e)** Photomicrograph of a biotite+sillimanite+garnet+K-feldspar+plagioclase+quartz migmatitic pelite with K-feldspar and quartz-plagioclase myrmekite (Myr) restricted to leucosome (10SRB-C235A) 2012-016. **f)** Outcrop photograph of garnetiferous granitic leucosome and biotite+sillimanite+garnet schollen; scale in centimetres (10SRB-H206A) 2012-019. Qtz = quartz, Kfs = K-feldspar, Grt = garnet, Sil = sillimanite, Bt = biotite.

into some pelite (Fig. 5d). Due to deformation, evidence for injection is typically definitive only if the granitoid vein is pegmatitic. The lack of migmatitic psammitic rocks suggests nonanatectic processes were subordinate to anatectic ones.

GRANULITE FACIES

Restricted areas throughout Cumberland Peninsula have granulite-facies mineral assemblages (Table 2), including metamorphic orthopyroxene in gabbro-diorite, orthopyroxene in psammite, and cordierite+garnet±K-feldspar in pelite (Fig. 2).

Cordierite+garnet±K-feldspar zone

Compared with sillimanite±K-feldspar zone pelite, the occurrence of cordierite coexisting with garnet (cordierite+garnet±K-feldspar zone) is typically accompanied by a reduced modal proportion, or virtual absence, of biotite (Fig. 6a), the occurrence of spinel, and an increase in the size of garnet, up to 7 cm in diameter. The characteristic mineral assemblages are cordierite+garnet+sillimanite±biotite± spinel±K-feldspar+plagioclase+quartz. Spinel is often present only as inclusions in garnet. Spinel in the matrix typically has an irregular shape and moats of sillimanite or garnet around it (Fig. 6a) suggesting spinel was partially replaced by sillimanite or garnet. Migmatitic textures are common and leucosome compositions are granitic to trondhjemitic (Fig. 6b, c).

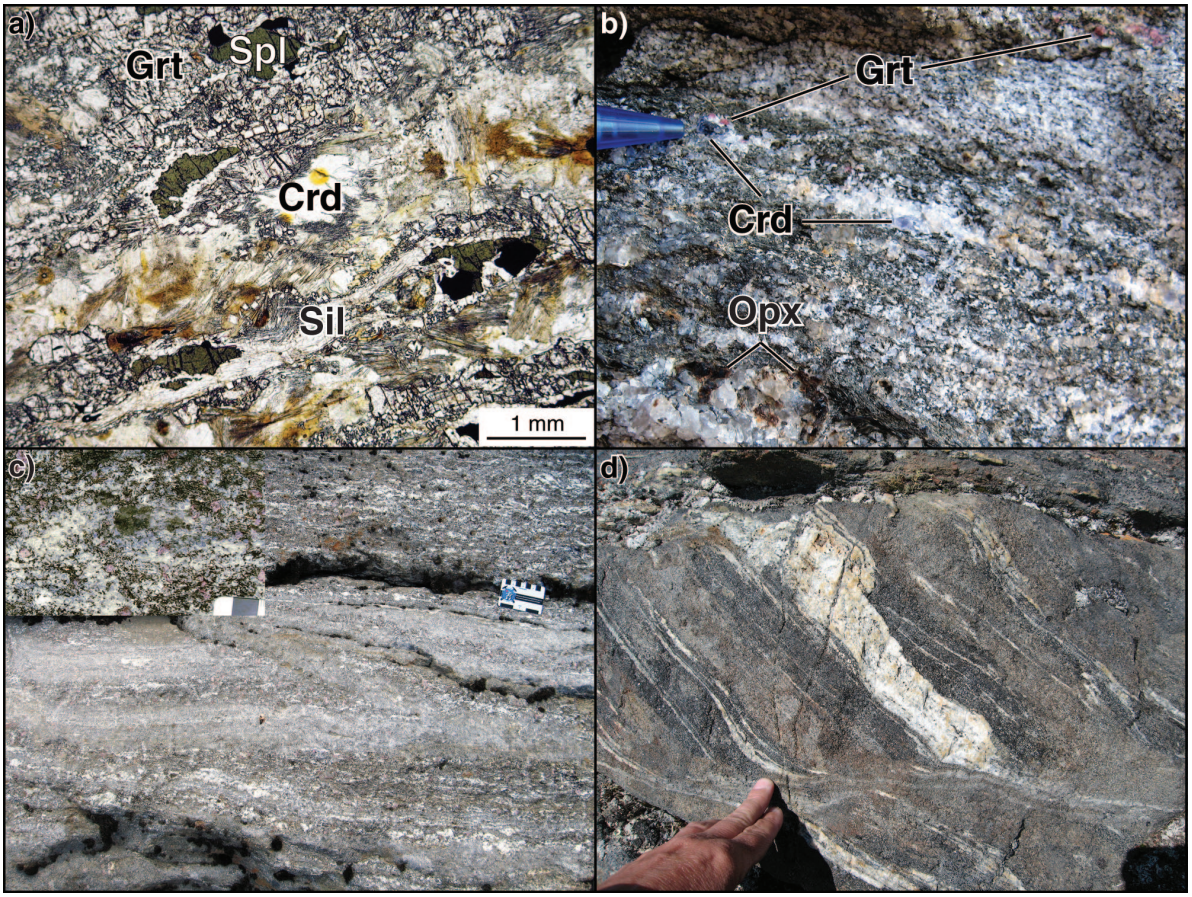

Figure 6. Granulite facies rocks from Cumberland Peninsula. **a)** Photomicrograph of a spinel+ cordierite+garnet+sillimanite+perthite+plagioclase+quartz pelite with minor biotite. Spinel is corroded with garnet or sillimanite moats and cordierite has sillimanite along grain boundaries, suggestive of partial replacement of both spinel and cordierite (10SRB-C199A) 2012-032. **b)** Outcrop photograph orthopyroxene+cordierite+garnet+anthophyllite+biotite+plagioclase+quartz semipelite. Pen tip for scale is 1.5 cm (09SRB-M036B) 2012-015. **c)** Photographs of a cordierite+garnet±K-feldspar zone migmatite outcrop. Darker coloured layers are pelitic and have leucosome; lighter coloured layers are psammitic and are not migmatitic. The inset photographs is a detailed view of a pelitic layer (09SRB-H116A) 2012-021, 2012-013. **d)** Outcrop photograph of gabbro cut by granitoid veins. The brown-weathering gabbro is orthopyroxene+hornblende-bearing, whereas black-weathering gabbro marginal to the granitoid veins is only hornblende-bearing; field of view is about 50 cm wide (09SRB-M032A) 2012-011. Grt = garnet, Spl = spinel, Crd = cordierite, Sil = sillimanite, Opx = orthopyroxene.

Cordierite±orthopyroxene is observed in a few localities (e.g. 09SRB-M036; Fig. 6b). In some localities, either or both these minerals occur in leucosome, but not in the matrix. In these cases, both minerals likely represent peritectic product phases formed by an incongruent melting reaction. For example, cordierite may have crystallized due to the reaction biotite+sillimanite+quartz±plagioclase = garnet+cordierite+liquid±K-feldspar (Pattison et al., 2003). Because these incongruent reactions define the lower boundary of the granulite facies in pelite, these localities are included in the cordierite+garnet± K-feldspar zone.

Kairolik Fiord granulite domain

A number of localities in the southeastern part of the peninsula preserve metamorphic orthopyroxene±clinopyroxene in gabbroic rocks (Fig. 6d) and orthopyroxene in tonalitic rocks. This region, designated the 'Kairolik Fiord granulite domain', is the only area with the assemblage clinopyroxene+garnet+hornblende+plagioclase+quartz in gabbroic rocks. In addition to granulite-facies rocks, it contains many localities with amphibolite-facies assemblages. Structures have not been identified that could account for the intermittent nature of the granulite-facies rocks; therefore, the Kairolik Fiord granulite domain is thought to locally preserve granulite-facies assemblages within a region that was partially retrogressed to amphibolite facies. An example of retrogression is seen in an orthopyroxene-bearing gabbroid that was hydrated to amphibolite in areas adjacent to granitoid veins (Fig. 6d).

MICROSTRUCTURES IN PELITIC ROCKS

Lower- and middle-amphibolite facies

In lower- and middle-amphibolite-facies pelitic rocks, mesoscopic folds typically plunge shallowly to the west and verge south and therefore correlate with regional F_2 folds. Only in the lower-grade rocks do some F_2 folds contain an axial-planar muscovite+biotite S_2 schistosity. Evidence for S_1 is restricted to F_2 fold hinges and if a single schistosity is present, it is assumed to be S_2. Large staurolite porphyroblasts are wrapped by S_2, and some contain straight inclusion trails at a high angle to this fabric. Smaller prismatic staurolite is generally oriented subparallel to S_2. Andalusite typically has straight inclusion trails at an angle to S_2 (Fig. 7a). Rarely, andalusite cores have straight inclusion trails, whereas rims have curved trails that are continuous with S_2 (Fig. 7b). Neither andalusite cores nor staurolite were observed with curved inclusion trails; therefore, growth of these porphyroblasts occurred after the formation of an early schistosity and prior to S_2. Andalusite rims indicate some andalusite growth occurred while S_2 was developing. Prismatic staurolite at a high angle to S_2 may indicate post-S_2 growth; however, these grains do not contain elongate inclusions.

Middle-amphibolite-facies garnet porphyroblasts preserve straight or curved internal fabrics at an angle to S_2 schistosity. One sample contains two matrix schistosities and straight inclusions in garnet are continuous with the earlier S_1 schistosity (Fig. 7c). These textures suggest that middle-amphibolite-facies garnet started growing while S_1 was developing and stopped before S_2 development began.

Upper-amphibolite facies

Oriented biotite and sillimanite, and compositional layering define the dominant foliation in upper-amphibolite-facies pelitic rocks. Mesoscopic folds are correlated with F_2 and evidence for S_1 is restricted to F_2 fold hinges (Fig. 7d). Minerals in F_2 fold hinges do not preserve evidence for intracrystalline strain (Fig. 7d) indicating the minerals recrystallized following folding. Upper-amphibolite-facies garnet is typically wrapped by S_2 and rarely includes a straight or curved fabric at an angle to the matrix schistosity. The development of S_2 outlasted the growth of garnet and curved inclusion trails in garnet were occluded during the development of either S_2 or an earlier fabric.

PRESSURE-TEMPERATURE CONDITIONS

Preliminary P-T constraints of the pelite mineral zones are derived using equilibrium assemblage diagrams (Fig. 8, 9, 10; Table 4). Three representative pelite compositions (Table 3) have been analyzed. Analysis of mineral compositions, necessary for a more complete analysis of P-T conditions, is in progress.

Lower- and middle-amphibolite facies

Any piezothermic array that includes each of the mineral assemblage zones must pass through the small staurolite+andalusite stability field (Fig. 8). If it is assumed that the peak P-T array defines a smooth curve, passage through this field requires a low P/T gradient. The sequence of mineral growth in samples from the sillimanite+muscovite zone (staurolite, andalusite, followed by sillimanite) indicates the prograde P-T path followed by these rocks also passed through the staurolite+andalusite field and had a shallow slope.

The staurolite+muscovite zone achieved peak conditions of about 530–575°C and 3.3–4.1 kbar. Chlorite-bearing samples were likely in the lower temperature end of this range. Andalusite+muscovite zone rocks reached a similar pressure with peak temperatures of less than approximately 610°C. The sillimanite+muscovite zone reached peak conditions

of 575–650°C with pressures greater than 3.5 kbar. A few pelitic rocks in the sillimanite+muscovite zone contain anomalously low-variance assemblages with staurolite, andalusite, and sillimanite. This is interpreted to reflect the upgrade persistence of andalusite and staurolite beyond their equilibrium terminal stability.

Upper-amphibolite facies

An equilibrium assemblage diagram for 09SRB-H090B (Fig. 9) is representative of rocks containing the widespread assemblage biotite+sillimanite+garnet+plagioclase+quartz. In the equilibrium assemblage diagram, muscovite is predicted to react out downgrade of the water-saturated solidus and K-feldspar is not predicted to be produced until temperatures greater than the water-saturated solidus, giving a broad P-T domain that contains the observed muscovite- and K-feldspar-free, locally migmatitic assemblage. The predicted reaction sequence is investigated along an example prograde P-T path (black line in Fig. 9). Muscovite is predicted to react out at temperatures below the water-saturated solidus via the continuous reaction

$$\text{muscovite+garnet} = \text{biotite+sillimanite+plagioclase+quartz+}H_2O, \quad (1)$$

producing the observed assemblage of biotite+garnet+sillimanite+plagioclase+quartz. Muscovite is completely consumed by Reaction 1 at 595°C along the example P-T path. Assuming little free water is contained along grain boundaries of the rock, the next significant reaction is a melt-forming reaction due to the continuous breakdown of biotite

$$\text{biotite+sillimanite+quartz} = \text{liquid+garnet}, \quad (2)$$

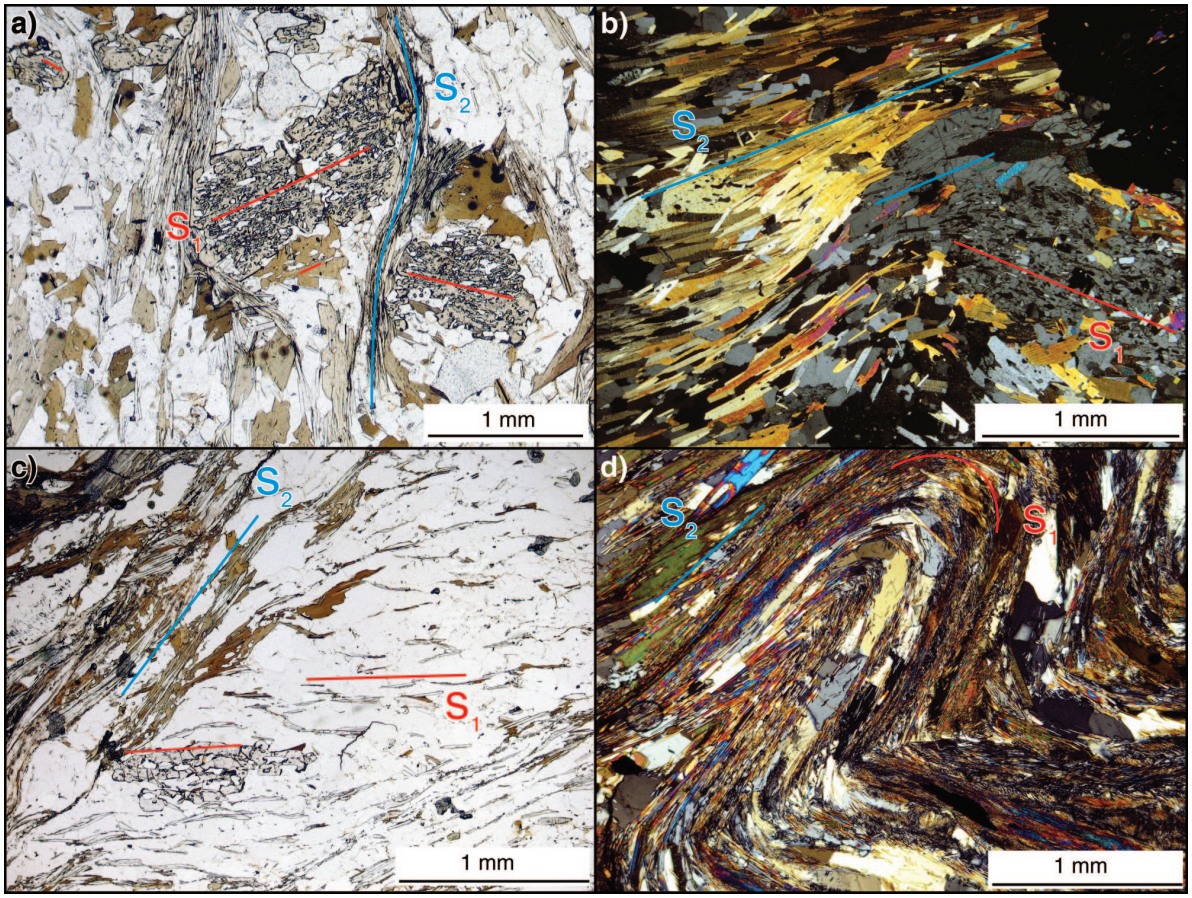

Figure 7. Representative microfabrics in amphibolite-facies pelite. **a)** Staurolite, with straight inclusion trails (S_1), is wrapped by the muscovite+biotite schistosity (S_2). Biotite in staurolite strain shadows also contains straight inclusion trails (S_1; staurolite+muscovite zone; 10SRB-Q039A) 2012-023. **b)** Straight inclusion trails in the core of an andalusite porphyroblast (S_1) are oblique to the muscovite and biotite schistosity (S_2), but curve at the edge of the crystal into parallelism with S_2 (lower-most sillimanite+muscovite zone; 10SRB-Y120B) 2012-028. **c)** Fine-grained muscovite schistosity (S_1) and coarser grained muscovite+biotite schistosity (S_2). A poikiloblastic garnet has straight inclusion trails parallel to, and continuous with S_1 (sillimanite+muscovite zone; 09SRB-M082C) 2012-014. **d)** Folding of an early biotite+sillimanite schistosity (S_1) produced open to isoclinal folds (F_2) with no axial-planar schistosity. Uniform extinction of quartz and unkinked sillimanite perpendicular to the axial-planar surface indicate recrystallization following folding (sillimanite±K-feldspar zone; 09SRB-D056A) 2012-058.

which begins at 675°C on the example P-T path. As biotite is consumed, the liberated potassium partitions between plagioclase and the liquid phase, but peritectic K-feldspar is not produced until 740°C. If the peak temperature remained below 740°C, back-reaction of the liquid with the matrix during cooling would prevent K-feldspar crystallization; however, chemical isolation of the liquid from the source would result in K-feldspar crystallizing from the liquid. Gradation between these end members may account for some of the range in K-feldspar development. The observed mineral assemblage suggests peak temperature was 595°C to 740°C. Evidence for partial melting, which is present in some, but not all rocks in this zone, indicates temperatures greater than 675°C locally.

Cordierite+garnet±K-feldspar zone

Preliminary thermodynamic modelling indicates cordierite+garnet±K-feldspar zone samples attained temperatures over 680°C (Fig. 8, 10). If the Fe^{3+}/Fe^{2+} ratio of spinel-bearing rocks is small, equilibrium temperatures could exceed 800°C (Fig. 10). Microtextures suggest that spinel and cordierite were partially replaced by sillimanite or garnet, and sillimanite, respectively, suggestive of down-temperature, but not down-pressure retrograde reactions (Fig. 10).

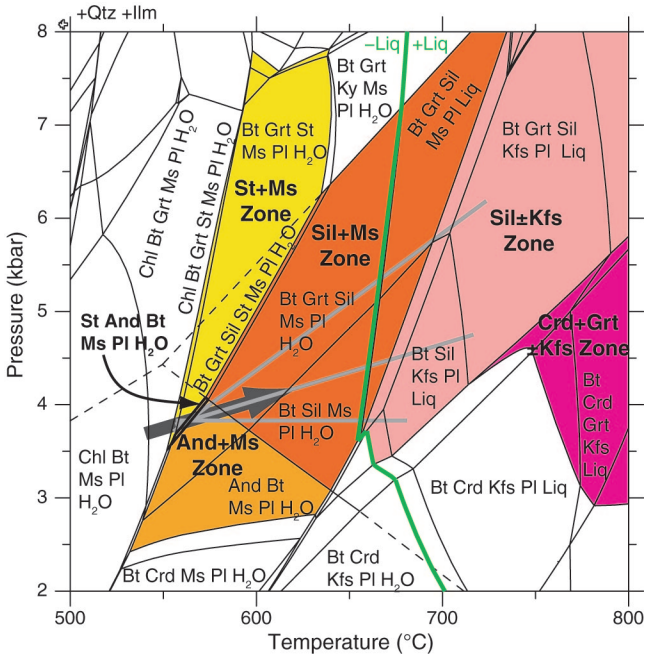

Figure 8. An MnNCKFMASHT equilibrium assemblage diagram for 09SRB-T085A (Table 3). Assemblage fields are coloured to correspond with the pelite zones on the Cumberland Peninsula metamorphic maps (Fig. 2, 3). Light grey lines represent possible piezothermic arrays satisfying the regional zonal sequence. The dark grey arrow is one possible prograde P-T path for the muscovite+sillimanite zone. Dashed lines are metastable Al_2SiO_5 phase boundaries. The staurolite+andalusite (+biotite+muscovite+plagioclase+quartz+ilmenite) stability field is outlined with thick black lines. Light grey lines represent possible piezothermic arrays that satisfy the regional zonal sequence. Qtz = quartz, Ilm = ilmenite, Chl = chlorite, Bt = biotite, Grt = garnet, Ms = muscovite, Pl = plagioclase, St = staurolite, Sil = sillimanite, Ky = kyanite, Kfs = K-feldspar, Crd = cordierite, And = andalusite, Liq = liquid.

Gabbroid granulite

Orthopyroxene-bearing metagabbro is stable at pressures below 10 kbar and temperatures in excess of 700°C to 850°C depending on pressure (Pattison et al., 2003). Clinopyroxene+garnet-bearing metagabbro occurs near

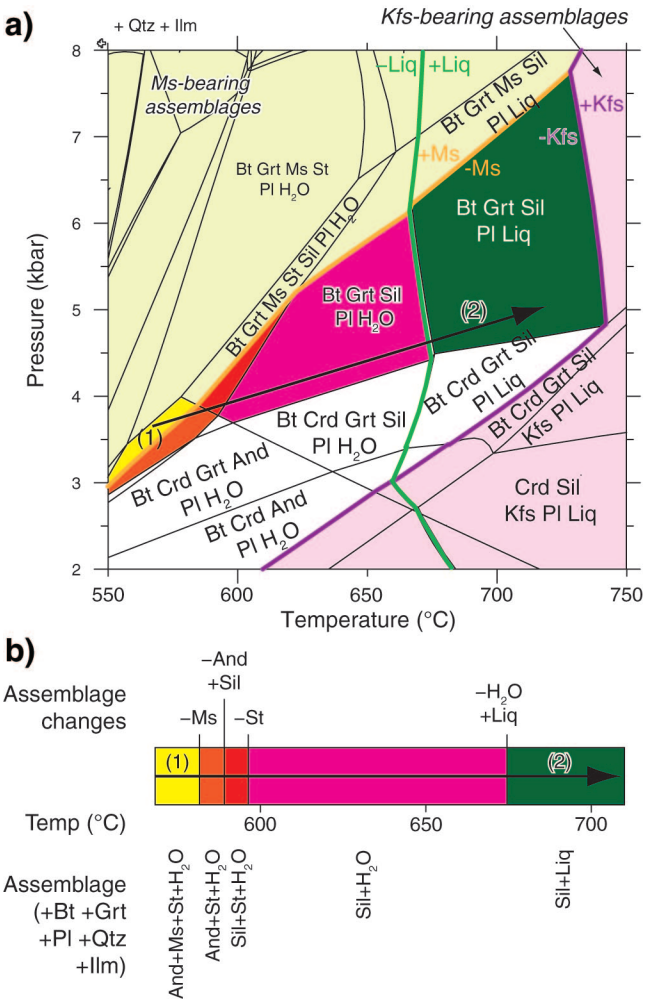

Figure 9. a) An MnNCKFMASHT equilibrium assemblage diagram for 09SRB-H090B (Table 3). The pastel yellow portion demarcates muscovite-bearing assemblages and pastel pink fields have K-feldspar. The black line is a hypothetical, but possible prograde P-T path for a sample in the sillimanite±K-feldspar zone. Equations 1 and 2, continuous reactions described in the text, take place in the fields labelled (1) and (2), respectively. **b)** The stable phases along the same prograde P-T path drawn in Figure 9a. The labelled lines that extend above the rectangle mark the appearance and disappearance of phases. Qtz = quartz, Ilm = ilmenite, Bt = biotite, Grt = garnet, Ms = muscovite, St = staurolite, Pl = plagioclase, Sil = sillimanite, Kfs = K-feldspar, Crd = cordierite, And = andalusite, Liq = liquid.

orthopyroxene-bearing rocks in the Kairolik Fiord granulite domain (Fig. 2). Although clinopyroxene+garnet gabbroid rocks occur at higher pressures elsewhere in the world (>10 kbar, 825–900°C; Pattison et al., (2003)), they may develop at lower pressures and temperatures (Pattison, 2003); therefore, they do not necessarily indicate high-pressure granulite-facies metamorphism.

DISCUSSION

Metamorphic events

The distribution of the metamorphic mineral zones suggests a polymetamorphic history involving episodes of early granulite-facies metamorphism (M_A), regional-contact (M_{P1}), and regional metamorphism (M_{P2}). The Kairolik Fiord granulite domain has granulite-facies assemblages that are thought to have formed during early granulite-facies metamorphism (M_A). An Archean pluton in the centre of the Kairolik Fiord granulite domain may be a heat source for granulite-facies metamorphism, but the domain is large compared to the size of the intrusion, suggesting either there are unexposed Archean plutons, or granulite-facies metamorphism was regional. A number of granulite-facies localities occur within 18 km of orthopyroxene-bearing plutons of the post-M_A Qikiqtarjuaq plutonic suite. The association of granulite-facies metamorphism with this batholithic complex suggests it was an important heat source responsible for regional-scale contact metamorphism (M_{P1}).

Regional metamorphism (M_{P2}) is indicated by the wide aerial extent of amphibolite-facies rocks. Retrogression from granulite-facies to amphibolite-facies in the Kairolik Fiord granulite domain is interpreted to be M_A followed by M_{P2}. There are a few cordierite+garnet±K-feldspar zone localities that are far from Qikiqtarjuaq plutonic suite plutons and the Kairolik Fiord granulite domain. These may be associated with unexposed plutons, or may indicate that M_{P2} locally obtained granulite facies (Fig. 2).

It is difficult to assess the extent of regional-contact metamorphism (M_{P1}) beyond granulite-facies localities because of the later amphibolite-facies overprint (M_{P2}). Garnetiferous granite and sillimanite±K-feldspar zone pelitic rocks with abundant leucosome occur near plutons of the Qikiqtarjuaq plutonic suite and the implied extensive partial melting is likely due to heat from these plutons. Mapping leucosome abundance may provide additional insight into the extent of M_{P1}.

Mesoscopic structures in Paleoproterozoic sedimentary rocks require at least two phases of Paleoproterozoic deformation. Most porphyroblasts overgrew a schistosity and were wrapped by a second schistosity, although there is local evidence for porphyroblast growth occurring while each schistosity was developing. Therefore, the majority of M_{P2} porphyroblast growth is interpreted to have occurred between the two deformational events.

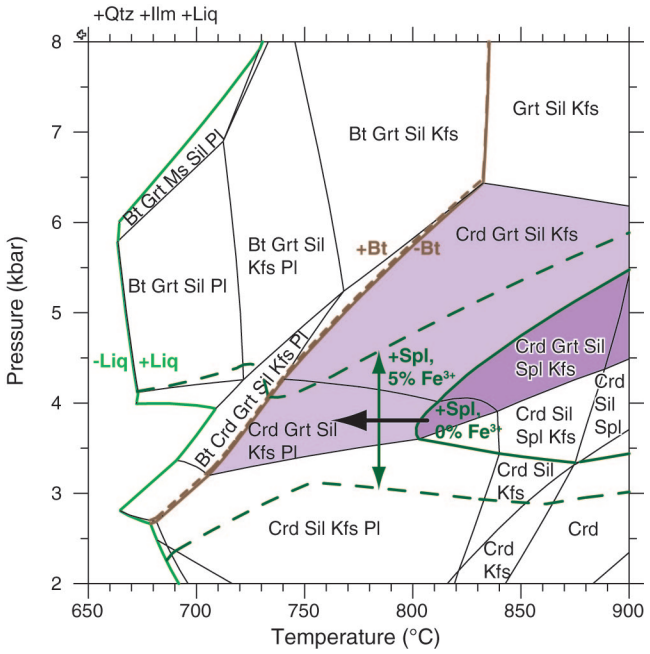

Figure 10. An MnNCKFMASHTO equilibrium assemblage diagram for 09SRB-H108B (Table 3) depicting the approximate P-T region for assemblages of the cordierite+garnet±K-feldspar zone. Solid lines were calculated with all iron as Fe^{2+} and dashed lines were calculated with 5% of the total iron as Fe^{3+}. The brown line marks the upper stability limit of biotite and the dark green line outlines the spinel stability region. The spinel+cordierite+garnet+sillimanite stability field (Fe^{3+} = 0) is dark violet and commonly observed cordierite+garnet+sillimanite (biotite-absent) assemblage is light violet. The bold black line is an approximate retrograde P-T path. Qtz = quartz, Ilm = ilmenite, Bt = biotite, Grt = garnet, Ms = muscovite, Sil = sillimanite, Pl = plagioclase, Kfs = K-feldspar, Crd = cordierite, Spl = spinel, Liq = liquid.

Origin of the Touak-Sunneshine metamorphic low

The origin of the Touak-Sunneshine metamorphic low is not fully understood. At three localities over a 55 km strike length the southern and/or southeastern boundary of the Touak-Sunneshine metamorphic low can be constrained to within 10 km of the north-dipping southern and/or southeastern fault contact between the Archean plutonic gneiss complex and the central Hoare Bay group belt. Its proximity

Table 4. Approximate pressure and temperature conditions for metamorphic zones.

Zone	Temperature (°C)	Pressure (kbar)
Staurolite+muscovite	530–575	3.3–4.1
Andalusite+muscovite	530–610	3.3–4.1
Sillimanite+muscovite	575–650	More than 3.5
Sillimanite±K-feldspar	More than 600	Poorly constrained
Sillimanite+K-feldspar	More than 650	Poorly constrained
Cordierite+garnet±K-feldspar	More than 680	3–8
P-T estimates were obtained from Figures 8–10.		

suggests that the metamorphic pattern might be related to faulting. The presence of lower grade rocks structurally and stratigraphically on top of higher grade rocks suggests faulting may have had a component of late- or postmetamorphic normal displacement; however, west-trending, mylonitic mineral lineations along the contact are subhorizontal, and there is no structural evidence for top to the north and/or northwest normal faulting.

The map pattern of the Touak-Sunneshine metamorphic low indicates it is a metamorphic synform; however, the metamorphic structure is not coincident with a comparable lithological synform. Because F_2 folding occurred after M_{P2} porphyroblast growth, it is plausible that the isograds developed after an early phase of deformation, and F_2 folding formed the synformal structure.

Timing of metamorphic events

Preliminary timing constraints available for Cumberland Peninsula, including new monazite geochronology (Hamilton et al., 2011; R.G. Berman, M. Sandborn-Barrie, B. Hamilton, N.M. Rayner, and M.D. Young, unpub. manuscript, 2012), support the relative chronology presented above. Monazite in pelite within the Kairolik Fiord granulite domain yielded ages of ca. 2.78 Ga, 2.70 Ga, and 1.8 Ga. Charnockitic and granodioritic plutons have been dated at ca. 2.77 Ga, 2.76 Ga, and 2.70 Ga (Rayner et al., in press) and and one monzogranite sample from the Archean plutonic gneiss complex that intruded sedimentary rocks has a crystallization age of 2.78 Ga (Rayner et al., in press), supporting a linkage between Neoarchean plutonism and M_A granulite-facies metamorphism in the Kairolik Fiord granulite domain. A number of phases of the Qikiqtarjuaq plutonic suite that are geochemically similar (Whalen et al., in press) yield crystallization ages between ca. 1.89 Ga and 1.88 Ga (Rayner et al., in press). Monazite from semipelite located 2.6 km from a Qikiqtarjuaq plutonic suite pluton yielded an overlapping age of ca. 1.895 Ga, supporting the interpretation of MP_1 regional-contact metamorphism. Monazite from pelite and semipelite in the area affected by M_{P2} regional metamorphism has a dominant age of ca 1.86 Ga, suggesting regional metamorphism postdated regional contact metamorphism.

Low-pressure regional metamorphism

The regional metamorphic facies series on Cumberland Peninsula is characterized by a progression from staurolite to andalusite with increasing grade. This facies series was termed the low-pressure intermediate group by Miyashiro (1961), and corresponds to facies series 2b (3.5–4.5 kbar) of Pattison and Tracy (1991). Regional metamorphism of the Touak-Sunneshine metamorphic low is similar to the low-pressure, andalusite-bearing regional metamorphism that characterizes much of the Trans-Hudson Orogen (Berman, 2010), together with several other Paleoproterozoic regional metamorphic terrains in the world (Grambling, 1981).

Regional andalusite+muscovite zone metamorphism requires a transient low-P, high-T geothermal gradient that is not predicted in thermal models of orogenic crustal thickening (e.g. England and Thompson, 1984). Proposed means of generating regional low-P, high-T conditions include crustal thickening combined with anomalously high crustal radiogenic heat production (Jamieson et al., 1998; Clark et al., 2011), asthenospheric upwelling (Loosveld and Etheridge, 1990; Sandiford and Powell, 1991), voluminous mid-crustal plutonism (Lux et al., 1986), or synmetamorphic rifting (Wickham and Oxburgh, 1985). Geological evidence for synmetamorphic rifting, such as normal faults or ductile extensional structures, mafic magmatism, synmetamorphic rift-related sediments, and evidence for rifting or transtension in nearby areas (Wickham and Oxburgh, 1985), are all lacking on Cumberland Peninsula.

Inferred Paleoproterozoic thick-skinned thrusting on Cumberland Peninsula would have caused crustal thickening. This horizontal shortening preceded regional metamorphism as is required by an orogenic thickening–radiogenic heating mechanism. Tectonic models for the region propose crustal thickening due to the ca. 1.88 Ga to 1.865 Ga collision between the Rae craton and the Meta Incognita microcontinent (St-Onge et al., 2007; Corrigan et al., 2009; Whalen et al., 2010). If orogenic thickening alone were to have produced the observed low-P, high-T metamorphic conditions, it would imply anomalously radiogenic mid- or lower-crust (Jamieson et al., 1998; Sandiford and Hand, 1998; Berman et al., 2010).

The intrusion of extensive charnockitic and granitic Qikiqtarjuaq plutonic suite magma would have increased the temperature of the mid-crust prior to regional metamorphism possibly facilitating low-P, high-T metamorphism during subsequent collision and crustal thickening. Unlike the cordierite+garnet±K-feldspar isograd, however, the middle-amphibolite-facies isograds are not subparallel to pluton margins, suggesting they are not directly related to Qikiqtarjuaq plutonic suite magmatism. Data presented in this paper is insufficient to assess if the Qikiqtarjuaq plutonic suite was a viable heat source.

Geological evidence for asthenospheric upwelling in the Paleoproterozoic exists in the Baffin Island region, but is lacking on Cumberland Peninsula. Magmas of the Cumberland Batholith (1.865–1.845 Ga; Whalen et al. (2010)) and the Prøven Igneous Complex (1.87 Ga; Thrane et al. (2005)), in southern Baffin Island, and Greenland, respectively, are thought to be a result of partial melting of the crust due to asthenospheric upwelling. Whereas the ages of these intrusions overlap the timing of regional metamorphism on Cumberland Peninsula, it is difficult to relate the two events given the absence of ca. 1.86 Ga plutons on Cumberland Peninsula.

ACKNOWLEDGMENTS

The authors wish to thank R. Berman, D. James, J. Percival, N. Rayner, M. St-Onge, J. Whalen, and N. Wodicka for discussions and B. Hillary for GIS support and handling of the manuscript. Assistance in the field was provided by E. Storey and the Cumberland Peninsula Multiple Metals project field crew, and the authors thank C. Nagy and R. Keim in particular. Funding for this project was provided through Natural Resources Canada's Geo-mapping for Energy and Minerals (GEM) program, Polar Continental Shelf Program (002-09, 014-10, 617-11), Canada-Nunavut Geoscience Office, Natural Sciences and Engineering Research Council of Canada Discovery Grant 037233 to D. Pattison, and an Alexander Graham Bell Canada Graduate Scholarship and the W. Garfield Weston Award for Northern Research (Doctoral) to B. Hamilton. The authors thank D. Moynihan, J. Cubley, and E. Webster for comments on an earlier version of the manuscript. This manuscript was significantly improved by a helpful and thorough review by R. Berman.

REFERENCES

Berman, R.G., 2010. Metamorphic map of the western Churchill Province, Canada; Geological Survey of Canada, Open File 5279, 3 sheets, 1:2 500 000 scale, + 49 p. doi:10.4095/287320

Berman, R.G., Sandeman, H.A., and Camacho, A., 2010. Diachronous Palaeoproterozoic deformation and metamorphism in the Committee Bay belt, Rae Province, Nunavut: insights from ^{40}Ar–^{39}Ar cooling ages and thermal modelling; Journal of Metamorphic Geology, v. 28, p. 439–457. doi:10.1111/j.1525-1314.2010.00873.x

Brown, M., 1973. The definition of metatexite, diatexite and migmatite; Proceedings of the Geologists' Association, v. 84, no. 4, p. 371–382.

Carmichael, D.M., 1969. On the mechanism of prograde metamorphic reactions in quartz-bearing pelitic rocks; Contributions to Mineralogy and Petrology, v. 20, p. 244–267. doi:10.1007/BF00377479

Clark, C., Fitzsimons, I.C.W., Healy, D., and Harley, S.L., 2011. How does the continental crust get really hot; Elements, v. 7, p. 235–240. doi:10.2113/gselements.7.4.235

Corrigan, D., Pehrsson, S., Wodicka, N., and de Kemp, E., 2009. The Palaeoproterozoic Trans-Hudson Orogen: a prototype of modern accretionary processes; *in* Ancient orogens and modern analogues, (ed.) J.B. Murphy, J.D. Keppie, and A.J. Hynes; Geological Society, London, Special Publications, v. 327, p. 457–479.

de Capitani, C. and Brown, T.H., 1987. The computation of chemical equilibrium in complex systems containing non-ideal solutions; Geochimica et Cosmochimica Acta, v. 51, p. 2639–2652. doi:10.1016/0016-7037(87)90145-1

de Capitani, C. and Petrakakis, K., 2010. The computation of equilibrium assemblage diagrams with Theriak/Domino software; The American Mineralogist, v. 95, p. 1006–1016. doi:10.2138/am.2010.3354

England, P.C. and Thompson, A.B., 1984. Pressure-temperature-time paths of regional metamorphism I. Heat transfer during the evolution of regions of thickened continental crust; Journal of Petrology, v. 25, no. 4, p. 894–928.

Fraser, J.A., Heywood, W.W., and Mazurski, M.A., 1978. Metamorphic map of the Canadian Shield; Geological Survey of Canada, Map 1475A, scale 1:3 500 000. doi:10.4095/133909

Grambling, J.A., 1981. Pressures and temperatures in Precambrian metamorphic rocks; Earth and Planetary Science Letters, v. 53, p. 63–68. doi:10.1016/0012-821X(81)90026-1

Hamilton, B.M., Sanborn-Barrie, M., Young, M.D., Pattison, D.R.M., Berman, R.G., and Rayner, N., 2011. Nature and timing of metamorphism and deformation on Cumberland Peninsula, Baffin Island, Nunavut; *in* Ottawa 2011, Geological Association of Canada–Mineralogical Association of Canada–Society of Economic Geologists–Society for Geology Applied to Mineral Deposits Joint Annual Meeting, Ottawa, Ontario; Geological Association of Canada, Abstracts Volume 34, p. 84.

Hoffman, P.F., 1988. United plates of America, the birth of a craton: Early Proterozoic assembly and growth of Laurentia; Annual Review of Earth and Planetary Sciences, v. 16, p. 543–603. doi:10.1146/annurev.ea.16.050188.002551

Holland, T.J.B. and Powell, R., 1998. An internally consistent thermodynamic data set for phases of petrological interest; Journal of Metamorphic Geology, v. 16, p. 309–343. doi:10.1111/j.1525-1314.1998.00140.x

Jackson, G.D., 1971. Operation Penny Highlands south-central Baffin Island; *in* Geological Survey of Canada, Paper 71-1, Part A, p. 138–140.

Jackson, G.D. and Morgan, W.C., 1978. Precambrian metamorphism on Baffin and Bylot Islands; *in* Metamorphism in the Canadian Shield, (ed.) J.A. Fraser and W.W. Heywood; Geological Survey of Canada, Paper 78-10, p. 249–267.

Jackson, G.D. and Taylor, F.C., 1972. Correlation of major Aphebian rock units in the northeastern Canadian Shield; Canadian Journal of Earth Sciences, v. 9, p. 1650–1669. doi:10.1139/e72-146

Jamieson, R.A., Beaumont, C., Fullsack, P., and Lee, B., 1998. Barrovian regional metamorphism: where's the heat? *in* What drives metamorphism and metamorphic reactions?, (ed.) P.J. Treloar and P.J. O'Brien; Geological Society, London, Special Publications, v. 138, p. 23–51.

Keim, R.D., Sanborn-Barrie, M., Ansdell, K., and Young, M., 2011. Totnes Road metavolcanic rocks: a fragmental, Ti-enriched komatiitic volcanic suite on Cumberland Peninsula, Baffin Island, Nunavut; Geological Survey of Canada, Current Research 2011-13, 22 p. doi:10.4095/289072

Loosveld, R.J.H. and Etheridge, M.A., 1990. A model for low-pressure facies metamorphism during crustal thickening; Journal of Metamorphic Geology, v. 8, p. 257–267. doi:10.1111/j.1525-1314.1990.tb00472.x

Lux, D.R., DeYoreo, J.J., Guidotti, C.V., and Decker, E.R., 1986. Role of plutonism in low-pressure metamorphic belt formation; Nature, v. 323, p. 794–797. doi:10.1038/323794a0

Miyashiro, A., 1961. Evolution of metamorphic belts; Journal of Petrology, v. 2, no. 3, p. 277–311.

Miyashiro, A., 1994. Metamorphic petrology; Oxford University Press, Inc., New York, New York, 404 p.

Pattison, D.R.M., 2003. Petrogenetic significance of orthopyroxene-free garnet + clinopyroxene + plagioclase ± quartz-bearing metabasites with respect to the amphibolite and granulite facies; Journal of Metamorphic Geology, v. 21, p. 21–34. doi:10.1046/j.1525-1314.2003.00415.x

Pattison, D.R.M. and Tracy, R.J., 1991. Phase equilibria and thermobarometry of metapelites; *in* Contact metamorphism, (ed.) D.M. Kerrick; Reviews in Mineralogy, v. 6, Mineralogical Society of America, Washington, D.C., p. 105–206.

Pattison, D.R.M., Chacko, T., Farquhar, J., and McFarlane, C.R.M., 2003. Temperatures of granulite-facies metamorphism: constraints from experimental phase equilibria and thermobarometry corrected for retrograde exchange; Journal of Petrology, v. 44, no. 5, p. 867–900. doi:10.1093/petrology/44.5.867

Rayner, N.M., Sanborn-Barrie, M., Young, M.D., and Whalen, J., in press. U-Pb ages of Archean basement and Paleoproterozoic plutonic rocks, southern Cumberland Peninsula, eastern Baffin Island; Geological Survey of Canada, Current Research 2012-8.

Sanborn-Barrie, M. and Young, M., 2011. Bulk compositional data for sulfidic and gossanous rocks from Cumberland Peninsula, Baffin Island, Nunavut; Geological Survey of Canada, Open File 6916, 11 p. doi:10.4095/288710

Sanborn-Barrie, M. and Young, M., in press a. Geology, Circle Lake, Nunavut; Geological Survey of Canada, Canadian Geoscience Map 5 (preliminary), scale 1:100 000.

Sanborn-Barrie, M. and Young, M., in press b. Geology, Durban Harbour, Nunavut; Geological Survey of Canada, Canadian Geoscience Map 37 (preliminary), scale 1:100 000.

Sanborn-Barrie, M. and Young, M., in press c. Geology, Padle Fiord, Nunavut; Geological Survey of Canada, Canadian Geoscience Map 38 (preliminary), scale 1:100 000.

Sanborn-Barrie, M., Young, M., and Whalen, J., 2011a. Geology, Kingnait Fiord, Nunavut; Geological Survey of Canada, Canadian Geoscience Map 2 (2nd edition, preliminary), scale 1:100 000. doi:10.4095/289238

Sanborn-Barrie, M., Young, M., Whalen, J., James, D., and St-Onge, M.R., 2011b. Geology, Touak Fiord, Nunavut; Geological Survey of Canada, Canadian Geoscience Map 3 (2nd edition, preliminary), scale 1:100 000. doi:10.4095/289239

Sanborn-Barrie, M., Young, M., Whalen, J., and James, D., 2011c. Geology, Ujuktuk Fiord, Nunavut; Geological Survey of Canada, Canadian Geoscience Map 1 (2nd edition, preliminary), scale 1:100 000. doi:10.4095/289237

Sanborn-Barrie, M., Young, M., Keim, R., and Hamilton, B., in press a. Geology, Sunneshine Fiord, Nunavut; Geological Survey of Canada, Canadian Geoscience Map 6 (preliminary), scale 1:100 000.

Sanborn-Barrie, M., Young, M., and Whalen, J.B., in press b. Geology, Qikiqtarjuaq, Nunavut; Geological Survey of Canada, Canadian Geoscience Map 39 (preliminary), scale 1:100 000.

Sandiford, M. and Hand, M., 1998. Australian Proterozoic high-temperature, low-pressure metamorphism in the conductive limit; *in* What drives metamorphism and metamorphic reactions? (ed.) P.J. Treloar and P.J. O'Brien; Geological Society, London, Special Publications, v. 138, p. 109–120.

Sandiford, M. and Powell, R., 1991. Some remarks on high-temperature – low-pressure metamorphism in convergent orogens; Journal of Metamorphic Geology, v. 9, p. 333–340. doi:10.1111/j.1525-1314.1991.tb00527.x

Sawyer, E.W. and Robin, P.Y.F., 1986. The subsolidus segregation of layer-parallel quartz-feldspar veins in greenschist to upper amphibolite facies metasediments; Journal of Metamorphic Geology, v. 4, p. 237–260. doi:10.1111/j.1525-1314.1986.tb00350.x

Spear, F.S., 1993. Metamorphic phase equilibria and pressure-temperature-time paths; Mineralogical Society of America, Washington, D.C., 799 p.

St-Onge, M.R., Wodicka, N., and Ijewliw, O., 2007. Polymetamorphic evolution of the Trans-Hudson Orogen, Baffin Island, Canada: integration of petrological, structural and geochronological data; Journal of Petrology, v. 48, no. 2, p. 271–302. doi:10.1093/petrology/egl060

Stowell, H., Bulman, G., Tinkham, D., and Zuluaga, C., 2011. Garnet growth during crustal thickening in the Cascades Crystalline Core, Washington, USA; Journal of Metamorphic Geology, v. 29, p. 627–647. doi:10.1111/j.1525-1314.2011.00933.x

Thrane, K., Baker, J., Connelly, J., and Nutman, A., 2005. Age, petrogenesis and metamorphism of the syn-collisional Prøven Igneous Complex, West Greenland; Contributions to Mineralogy and Petrology, v. 149, p. 541–555. doi:10.1007/s00410-005-0660-0

Whalen, J.B., Wodicka, N., Taylor, B.E., and Jackson, G.D., 2010. Cumberland Batholith, Trans-Hudson Orogen, Canada: Petrogenesis and implications for Paleoproterozoic crustal and orogenic processes; Lithos, v. 117, p. 99–118. doi:10.1016/j.lithos.2010.02.008

Whalen, J., Sanborn-Barrie, M., and Young, M., in press. Geochemical data from Archean and Paleoproterozoic plutonic and volcanic rocks of Cumberland Peninsula, eastern Baffin Island, Nunavut; Geological Survey of Canada, Open File 6933, 15 p. doi:10.4095/291453

Wickham, S.M. and Oxburgh, E.R., 1985. Continental rifts as a setting for regional metamorphism; Nature, v. 318, p. 330–333. doi:10.1038/318330a0

Geological Survey of Canada Project MGM 007